Modeling the Interactions between Peptide Functions and Cu(I): Formamide−Cu$^+$ Reactions in the Gas Phase

A. Luna,[†] B. Amekraz,[†] J. Tortajada,*,[†] J. P. Morizur,[†] M. Alcamí,[‡] O. Mó,[‡] and M. Yáñez*,[‡]

Contribution from the Laboratoire de Chimie Organique Structurale, Université Pierre et Marie Curie, CNRS UMR 172, Boite 45, 4 Place Jussieu, F-75252 Paris Cedex 05, and Departamento de Química, C-9, Universidad Autónoma de Madrid, Cantoblanco, 28049-Madrid, Spain

Abstract: The gas-phase reactions between Cu$^+$ and formamide, as the most simple model of a peptide function, have been investigated through the use of mass spectrometry techniques. The primary products formed in the ion source correspond mainly to three types of complexes: (i) those formed by direct interaction of Cu$^+$ with formamide: [formamide-Cu]$^+$, [(formamide)$_2$Cu]$^+$ complexes, (ii) secondary products generated by association of these ions with ammonia: [formamide-Cu-NH$_3$]$^+$ complexes, (iii) secondary products formed by interactions of [Cu$_2$H]$^+$ clusters with residual HNCO coming from the formamide-Cu$^+$ complexes elimination, namely [HNCO,Cu$_2$H]$^+$ species. The structures and bonding characteristics of these systems were studied by means of the B3LYP DFT approach. The [formamide-Cu]$^+$ potential energy surfaces were studied at the B3LYP/ 6-311+G(2df,2p) level in order to explore the validity of formamide to model peptidic reactivity with respect to Cu$^+$. This survey shows that the attachment of Cu$^+$ takes place preferentially at the carbonyl group, while attachment at the amino leads to a local minimum which lies 21 kcal/mol higher in energy. The estimated formamide−Cu$^+$ binding energy (56.2 kcal/mol) is equal to that previously reported for ammonia, although its intrinsic basicity with respect to H$^+$ is 7 kcal/mol smaller. The MIKE spectra of the different primary ions formed in the reaction have also been analyzed. For the particular case of formamide, CAD spectra have been also performed in order to have a more complete description of its reactivity. Starting from the [formamide-Cu]$^+$ complexes, several reaction channels leading to the loss of Cu$^+$, H$_2$O, NH$_3$, HCO, and HCN/CNH have been considered.

Introduction

Over the past few years, the study of gas-phase organometallic ion chemistry has experienced a rapid growth.[1-5] A wide variety of experimental techniques[3,6-9] was employed not only to determine the gas-phase binding energies of organic molecules to metal cations[10-12] but also to investigate the reactions which can occur as a consequence of the ion−neutral interaction. Very often the metal cation association implies a drastic reorganization of the charge density of the neutral which results in the activation of some particular bonds.[5] Hence, it is normal to observe, under normal experimental conditions, the spontaneous fragmentation of the ion−neutral complex.[5] These dissociative processes may be characteristic of some specific functional groups or kinds of compounds, which confers analytical utility to these techniques. Furthermore, collision-induced dissociation processes either of the neutral−ion complex or of some of the primary products formed in the spontaneous unimolecular decompositions may provide further information on the structure and bonding characteristics of the neutral and on some features of the Potential Energy Surface (PES). In this respect, it should be mentioned that Collision-Activated Dissociation (CAD) was found to be a very useful tool to investigate the amino acid sequence of peptides.[13-15] Also recently, Amster and co-workers[16,17] have used metal cation laser

* Corresponding authors: Dr. Jeanine Tortajada (telephone, 33 (1) 44 27 31 10; fax, 33 (1) 44 27 25 68; e-mail, jeat@moka.ccr.jussieu.fr) and Dr. Manuel Yáñez (telephone, 34 (1) 397 49 53; fax, 34 (1) 397 41 87; e-mail, manuel.yanez@uam.es).

† Université Pierre et Marie Curie.

‡ Universidad Autónoma de Madrid.

(1) Taft, R. W.; Tompson, R. D. *Prog. Phys. Org. Chem.* **1987**, *16*, 1.

(2) *Gas-Phase Ion Chemistry*; Bowers, M. T., Ed.; Academic Press: New York, 1979; Vols. 1 and 2, 1984; Vol. 3.

(3) *Fourier Transform Mass Spectrometry, Evolution, Innovation and Application*; Buchanan, M. V., Ed.; ACS Symposium Series 359; American Chemical Society: Washington, DC, 1987.

(4) See for instance: Armentrout, P. B.; Baer, T. *J. Phys. Chem.* **1996**, *100*, 12866, and references therein.

(5) *Organometallic Ion Chemistry*; Freiser B. S., Ed.; Kluwer Academic Publishers: Dordrecht, 1995.

(6) Ervin, K. M.; Armentrout, P. B. *J. Chem. Phys.* **1985**, *83*, 166.

(7) Sunderlin, L. S.; Wang, D.; Squires, R. R. *J. Am. Chem. Soc.* **1992**, *114*, 2788.

(8) Khan, F. A.; Clemmer, D. E.; Schultz, R. H.; Armentrout, P. B. *J. Phys. Chem.* **1993**, *97*, 7978.

(9) Hettich, R. L.; Jackson, T. C.; Stanko, E. M.; Freiser, B. S. *J. Am. Chem. Soc.* **1986**, *108*, 5086.

(10) Gal, J.-F.; Taft, R. W.; McIver, R. T. Jr. *Spectrosc. Int. J.* **1984**, *3*, 96.

(11) Operti, L.; Tews, E. C.; Freiser, B. S. *J. Am. Chem. Soc.* **1988**, *110*, 3847.

(12) Taft, R. W.; Anvia, F.; Gal, J.-F.; Walsh, S.; Capon, M.; Holmes, M. C.; Hosn, K.; Oloumi, G.; Vasanwala, R.; Yazdani, S. *Pure Appl. Chem.* **1990**, *62*, 17.

(13) (a) Johnson, R. S.; Biemann, K. *Biochemistry.* **1987**, *26*, 1209. (b) Biemann, K.; Scole, M. A.; *Science* **1987**, *237*, 992.

(14) Johnson, R. S.; Martin, S. A.; Biemann, K. *Int J. Mass. Spectrom. Ion Processes* **1988**, *86*, 137.

(15) Senko, M. W.; Speir, J. P.; McLafferty, F. W. *Anal. Chem.* **1994**, *66*, 2801.

(16) Speir, J. P.; Gorman, G. S.; Amster, I. J. *J. Am. Soc. Mass. Spectrom.* **1993**, *4*, 106.

(17) Lei, Q. P.; Amster, I. J. *J. Am. Soc. Mass Spectrom.* **1996**, *7*, 722.

desorption chemical ionization techniques for this purpose. The formation and fragmentation of amino acids complexed by Cu^+ have also been recently studied.[18,19]

In the past few years our research groups have focused their efforts in the investigation, both from the experimental and the theoretical points of view, of ion–molecule reactions involving small bases[20] of biochemical significance either because they are basic constituents of larger biochemical molecules or because they present active functional groups similar to the larger biochemical compounds. In this way it is possible to model the reactivity of more complicated biochemical systems, difficult to treat, at least from a theoretical point of view, due to their size.

The aim of this paper is to investigate the reactions in the gas-phase between formamide and Cu^+. Formamide can be considered as the simplest prototype of a peptide linkage. Actually its protonation was the subject of great interest because it can be used as a model to understand the proton exchange processes in peptides or proteins[21] or the hydrolysis of peptides bonds in living systems.[22] Furthermore, formamide is a typical bidentate base which permits the competition between N- and O-association to be investigated. Recently,[20a] we have investigated its interaction with Li^+, Na^+, Mg^+, and Al^+ metal monocations in an effort to investigate their possible catalytic role in the isomerization processes of this neutral. The interaction with transition metal monocations as Cu^+ has some specific and interesting peculiarities.[20f,23,24] First, the nature of the interaction is likely different from that found in the protonation processes, which lead to the formation of typical covalent bonds, and from those observed with the alkali metal monocations or Mg^+ and Al^+, where the interactions are essentially electrostatic. On the other hand, from the biological perspective, the Cu^+ reactions also play an important role.[17,25] In this respect it should be mentioned that relative and absolute Cu^+ basicity scales for the α-amino acids have been reported very recently in the literature.[26,27]

In this paper we shall first discuss the most important features of the Chemical Ionization–Fast-Atom Bombardment (CI–

FAB) mass spectrum that result from the reactions of Cu^+ with formamide, to characterize the primary products of the reactions which occur in the ion source. Then, the most significant ion products will be mass selected in order to investigate their spontaneous unimolecular dissociation by Mass-analyzed Ion Kinetic Energy (MIKE) spectrometry. As we are particularly interested in the reactivity of Cu^+–formamide adducts, we have also investigated the collision-activated evolution of this system by means of the CAD spectrum. The rationalization of the most outstanding experimental features would require a good knowledge of the corresponding PES which will be explored through the use of density functional theory approaches using large enough basis sets, to ensure the reliability of the calculated structures and energies.

The structure of this paper will then be as follows: after the statement of the experimental and theoretical methods, we will describe the FAB ion source spectrum resulting from the reactivity of Cu^+ with formamide. Some of the products observed in this spectrum have been investigated in detail, so for each of them the MIKE spectrum is presented and discussed, followed by a theoretical interpretation of the results in each case.

Experimental Section

All experiments were conducted using a VG Analytical ZAB–HSQ hybrid mass spectrometer[28] of BEqQ geometry. Complexes were generated by the CI–FAB method.[29] The CI–FAB source was constructed from VG Analytical EI/CI and FAB ion source parts with the same modifications described by Freas et al.[29a] The conventional FAB probe tip has been replaced by a foil of high purity of copper. "Naked" metal ions were generated by bombardment with fast xenon atoms (Xe gas 7−8 keV kinetic energy, 1−2 mA of emission current in the FAB gun). It can be noticed that, as it has been reported in the literature,[30] and in accordance with our results, this procedure yields Cu^+ ions as well as $[Cu_{(2n)}]^+$ and $[Cu_{(2n+1)}]^+$ cluster ions. $^{63}Cu^+$ and $^{65}Cu^+$ ions are produced in a ratio which is close to that of their natural abundance (100/44 versus 100/45, respectively). In contrast, an isotopic effect[30] is observed for the formation of cluster ions. As a consequence, in the case of Cu_2^+ and Cu_3^+ the difference between the experimental intensities and their statistical contributions is apparent. The Cu_2^+ clusters contain three ions at m/z 126, 128, and 130 in a ratio 96/100/33 versus 100/83/17 that should be statistically expected. For Cu_3^+ clusters the experimental abundance ratios for ions at m/z 189, 191, 193, and 195 (79/100/75/11) also differ from the statistical ones (71/100/37/7). These remarks must be taken into account when explaining the relative ion abundances resulting from the reactivity of these clusters toward neutral species for further studies.

The organic samples were introduced via a heated inlet system at 100 °C in a nonheated source. As mentioned by Schwarz et al.,[29e] we can assume that due to the relatively high pressure in the ion source ($10^{-2}-10^{-3}$ Pa), efficient collisional cooling of the ions takes place and therefore excited states of the Cu^+ ions are not likely to participate in the observed reactivity. The metal ion adduct complexes formed with the formamide were mass selected (using an acceleration voltage of 8 kV) with the magnetic analyzer B. Metastable and collision-activated dissociations occurring in the second field-free region (2nd FFR) between the magnetic and the electric analyzers were monitored

(18) (a) Wen, D.; Yalcin, T.; Harrison, A. G. *Rapid Commun. Mass Spectrom.* **1995**, *9*, 1155. (b) Bouchonnet, S.; Hoppilliard, Y.; Ohanessian, G. *J. Mass. Spectrom.* **1995**, *30*, 172.

(19) Lavanant, H.; Hoppilliard, Y. *J. Mass. Spectrom.* **1997**, *32*, 1037.

(20) (a) Tortajada, J.; Leon, E.; Morizur, J. P.; Luna, A.; Mó, O.; Yáñez, M. *J. Phys. Chem.* **1995**, *99*, 13890. (b) Amekraz, B.; Tortajada, J.; Morizur, J. P.; González, A. I.; Mó, O.; Yáñez, M.; Leito, I.; Maria, P.-C.; Gal, J.-F. *New J. Chem.* **1996**, *20*, 1011. (c) Amekraz, B.; Tortajada, J.; Morizur, J. P.; González, A. I.; Mó, O.; Yáñez, M. *J. Mol. Struct (THEOCHEM)* **1996**, *371*, 313. (d) González, A. I.; Mó, O.; Yáñez, M.; Leon, E.; Tortajada, J.; Morizur, J. P.; Leito, I.; Maria, P.-C.; Gal, J.-F. *J. Phys. Chem.* **1996**, *100*, 10490. (e) Leon, E.; Amekraz, B.; Tortajada, J.; Morizur, J. P.; González, A. I.; Mó, O.; Yáñez, M. *J. Phys. Chem. A* **1997**, *101*, 2489. (f) Luna, A.; Amekraz, B.; Morizur, J. P.; Tortajada, J.; Mó, O.; Yáñez, M. *J. Phys. Chem. A* **1997**, *101*, 5931.

(21) Perrin, C. I. *Acc. Chem. Res.* **1989**, *22*, 286 and references therein.

(22) Antonczak, S.; Ruiz-López, M. F.; Rivail, J. L. *J. Am. Chem. Soc.* **1994**, *116*, 3912 and references therein.

(23) Freiser, B. E. *J. Mass. Spectrom.* **1996**, *31*, 703. (b) Magnera, T. F.; David, D. E.; Stulik, D.; Orth, R. G.; Jonkman, H. T.; Michl, J. *J. Am. Chem. Soc.* **1989**, *111*, 5036.

(24) (a) Rosi, M.; Bauschlicher, C. W. *J. Chem. Phys.* **1989**, *90*, 7264. (b) Rosi, M.; Bauschlicher, C. W. *J. Chem. Phys.* **1990**, *92*, 1876. (c) Partridge, H.; Bauschlicher, C. W. *J. Phys. Chem.* **1994**, *98*, 2301. (d) Bauschlicher, C. W.; Langhoff, S. R.; Partridge, H. *J. Chem. Phys.* **1991**, *94*, 2068.

(25) (a) Karlin, K. D., Tyeklar, Z., Eds. *Bioinorganic Chemistry of Copper*; Chapman & Hall: New York, 1993. (b) Karlin, K. D.; Zubieta, J. *Biological and Inorganic Copper Chemistry*; Adenine: Guilderland, NY, 1986; Vols. I and II. (c) Karlin, K. D., Zubieta, J., Eds. *Copper Coordination Chemistry: Biological and Inorganic Perspectives*; Adenine: Guilderland, NY, 1983.

(26) Cerda, B. A.; Wesdemiotis, C. *J. Am. Chem. Soc.* **1995**, *117*, 9734.

(27) Hoyau, S.; Ohanessian, G. *J. Am. Chem. Soc.* **1997**, *119*, 2016.

(28) Harrison, A. G.; Mercer, R. S.; Reiner, E. J.; Young, A. B.; Boyd, R. K.; March, R. E.; Porter, C. J. *Int. J. Mass Spectrom. Ion Processes* **1986**, *74*, 13.

(29) (a) Freas, R. B.; Ross, M. M.; Campana, J. E. *J. Am. Chem. Soc.* **1985**, *107*, 6195. (b) Freas, R. B.; Campana, J. E. *J. Am. Chem. Soc.* **1985**, *107*, 6202. (c) Mestdagh, H.; Morin, N.; Rolando, C. *Tetrahedron Lett.* **1986**, *27*, 33. (d) Drewello, T.; Eckart, K.; Lebrilla, C. B.; Schwarz, H. *Int. J. Mass Spectrom. Ion Processes* **1987**, *76*, 13. (e) Hornung, G.; Schröder, D.; Schwarz, H. *J. Am. Chem. Soc.* **1995**, *117*, 8192. (f) Chamot-Rooke, J.; Tortajada, J.; Morizur, J.-P. *Eur. Mass Spectrom.*, **1995**, *1*, 471.

(30) Wang, G.; Dou, L.; Liu, Z.; Zhao, T.; Jiang, Y.; Yang, J. *Phys. Rev. B* **1988**, *37*, 9093.

by scanning the latter one. The metastable ion reactions were studied by MIKES[31a] techniques. CADs[31b] were performed by admitting argon as target gas into the second drift region collision cell to reduce the parent ion signal to 70%. The spectra were recorded at a resolving power (*R*) of ∼1000.

Formamide was purchased from Aldrich and used without further purification.

Computational Details

The theoretical treatment of the different systems included in this work was performed by using the B3LYP density functional approach[32] in the Gaussian-94 series of programs.[33] This method has been found to be quite reliable as far as the description of metal cation−neutral complexes is concerned,[34,20c,e,f] in particular when Cu⁺ ions are involved.[34,20f] The B3LYP approach is a hybrid method which includes the Becke's three-parameter nonlocal exchange potential[32] with the nonlocal correlation functional of Lee, Yang, and Parr.[35] The geometries of the different species under consideration were optimized using the all-electron basis of Watchers-Hay[36] for Cu and the 6-311G(d,p) basis set for the remaining atoms of the system. The harmonic vibrational frequencies of the different stationary points of the PES have been calculated at the same level of theory used for their optimization in order to identify the local minima and the transition states (TS), as well as to estimate the corresponding zero point energies (ZPE). To identify which minima are connected by a given TS, we have performed intrinsic reaction coordinate (IRC)[37] calculations at the same level of theory.

As mentioned above, we have shown[34a] that association energies for Cu⁺ complexes obtained at the B3LYP/6-311+G(2df,2p) level are in reasonably good agreement with those estimated in the framework of the G2 theory.[38] Hence, the final energies of the different species under study were obtained in B3LYP/6-311+G(2df,2p) single-point calculations at the aforementioned B3LYP/6-311G(d,p) optimized geometries. It should be noted that the basis set employed in these DFT calculations differs from that used in the G2 formalism in the number of sets of *d* polarization functions included. We have tested, however, taking the NH₃−Cu⁺ complexes as a suitable benchmark case, that the binding energies so obtained do not differ significantly from those calculated with the larger basis set, while the time of calculation is considerably reduced.

To investigate the bonding characteristics of the different species, we used the Atoms in Molecules (AIM) theory of Bader.[39] For this purpose we have located the bond critical points, i.e., points where the electron density function, $\rho(\mathbf{r})$, is minimum along the bond path and maximum in the other two directions. The Laplacian of the density, $\nabla^2\rho(\mathbf{r})$ identifies regions of the space wherein the electronic charge is locally depleted ($\nabla^2\rho > 0$) or built up ($\nabla^2\rho < 0$). The former situation is typically associated with interactions between closed-shell systems (ionic bonds, hydrogen bonds, and van der Waals molecules), while
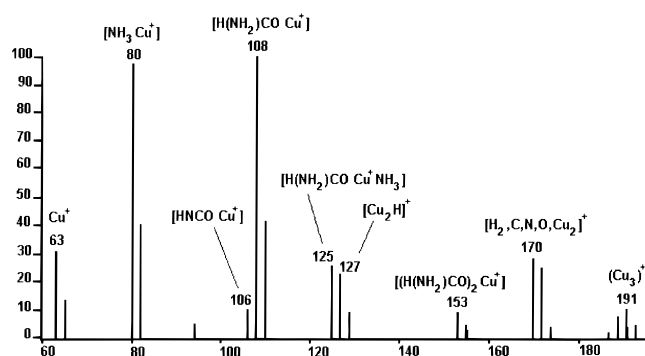
(31) (a) Cooks, R. G.; Beynon, J. H.; Caprioli, R. M.; Lester, G. R. *Metastable Ions*; Elsevier: New York, 1973. (b) *Collision Spectroscopy*; Cooks, R. G., Ed.; Plenum Press: New York, 1978.

(32) (a) Becke, A. D. *J. Chem. Phys.* **1993**, *98*, 5648. (b) Becke, A. D. *J. Chem. Phys.* **1992**, *96*, 2155.

(33) Frisch, M. J.; Trucks, G. W.; Schlegel, H. B.; Gill, P. M. W.; Johnson, B. J.; Robb, M. A.; Cheeseman, J. R.; Keith, T. A.; Peterson, G. A.; Montgomery, J. A.; Raghavachari, K.; Al-Laham, M. A.; Zakrzewski, V. G.; Ortiz, J. V.; Foresman, J. B.; Cioslowski, J.; Stefanow, B. B.; Nanayaklara, A.; Challacombe, M.; Peng, C. Y.; Ayala, P. Y.; Chen, W.; Wong, M. W.; Andres, J. L.; Replogle, E. S.; Gomperts, R.; Martin, R. L.; Fox, D. J.; Binkley, J. S.; Defrees, D. J.; Baker, J.; Stewart, J. P.; Head-Gordon, M.; Gonzalez, C.; Pople, J. A.; *Gaussian 94*; Gaussian, Inc.: Pittsburgh, PA, 1995.

(34) (a) Luna, A.; Amekraz, B.; Tortajada, J. *Chem. Phys. Lett.* **1997**, *266*, 31. (b) Hoyau, S.; Ohanessian, G. *Chem. Phys. Lett.* **1997**, *280*, 266.

(35) Lee, C.; Yang, W.; Parr, R. G. *Phys Rev.* **1988**, *B37*, 785.

(36) (a) Watchers, A. J. H. *J. Chem. Phys.* **1970**, *52*, 1033. (b) Hay, P. J. *J. Chem. Phys.* **1977**, *66*, 4377.

(37) González, C.; Schlegel, H. B. *J. Chem. Phys.* **1989**, *90*, 2154.

(38) Curtiss, L. A.; Raghavachari, K.; Trucks, G. W.; Pople, J. A. *J. Chem. Phys.* **1991**, *94*, 7221.

(39) Bader, R. F. W. *Atoms in Molecules. A Quantum Theory*; Oxford University Press: Oxford, 1990.

Figure 1. Mass spectrum that results from the reactions of Cu⁺ sputtered from a copper foil, with neutral formamide.

the latter characterizes covalent bonds, where the electron density concentrates in the internuclear region. There are however significant exceptions to this general rule, mainly when high electronegative atoms are involved in the bonding. Hence, we have also evaluated the energy density,[40] $H(\mathbf{r})$, which does not present these exceptions. In general, negative values of $H(\mathbf{r})$ are associated with a stabilizing charge concentration within the bonding region. The AIM analysis was performed using the AIMPAC series of programs.[41]

Results and Discussion

Figure 1 shows the mass spectrum that results from the gas-phase reactions of copper ions with formamide. The existence of ⁶³Cu and ⁶⁵Cu isotopes leads to an easy identification of copper-containing ions, as mentioned above. In our ion−molecule reaction conditions, besides production of Cu⁺, we have also observed the formation of copper cluster ions such as (Cu₃)⁺. No even-numbered species (Cu₂)⁺ were observed as has been already reported by Freas and Campana.[29b] However, cluster ions (Cu₂H)⁺ at *m/z* 127 (11%) were produced, whereas (Cu₂ₙ₊₁H)⁺ species were not detected. The abundance of the Cu⁺ species (32%) was greater than that of the large clusters (Cu₃)⁺ (*m/z* 191 8%) as shown in the mass spectrum of Figure 1.

Several copper/organic product complexes were observed in the mass spectrum. The Cu⁺ ions react with neutral formamide to produce mainly [formamide-Cu⁺] adduct ion at *m/z* 108 (100%). This complex in turn reacts with another formamide molecule to produce [(formamide)₂Cu⁺] at *m/z* 153 (9%). Formation of [formamide-Cu⁺-NH₃] at *m/z* 125 (26%) arises from the interaction of formamide with CuNH₃⁺ complexes formed by the spontaneous decomposition of formamide−Cu⁺ ions or alternatively by the association of formamide−Cu⁺ complexes with one molecule of ammonia, which, as we shall see later, is another product of the dissociation of formamide−Cu⁺ ions. The formation of [(formamide)₂Cu⁺] and [formamide-Cu⁺-NH₃] complexes reflects the ability of Cu⁺ to form dicoordinated species.[20f,23,24]

It is worth noting that two species contribute to the peak at *m/z* 127, namely [formamide-⁶⁵Cu⁺-NH₃] complexes and ⁶³Cu₂H⁺ clusters. According to the relative abundances discussed before, they should contribute equally to the observed peak intensity.

The detected Cu⁺ product ions containing formamide fragments were [NH₃Cu]⁺ at *m/z* 80 (98%) and [HNCOCu]⁺ at *m/z* 106 (11%). The (Cu₂H)⁺ ion appears to be chemically active

(40) (a) Cremer, D.; Kraka, E. *Chimica Acta* **1984**, *57*, 1529. (b) Cremer, D.; Kraka, E. *Angew. Chem., Int. Ed. Engl.* **1984**, *23,* 627.

(41) The AIMPAC programs package has been provided by J. Cheeseman and R. F. W. Bader.
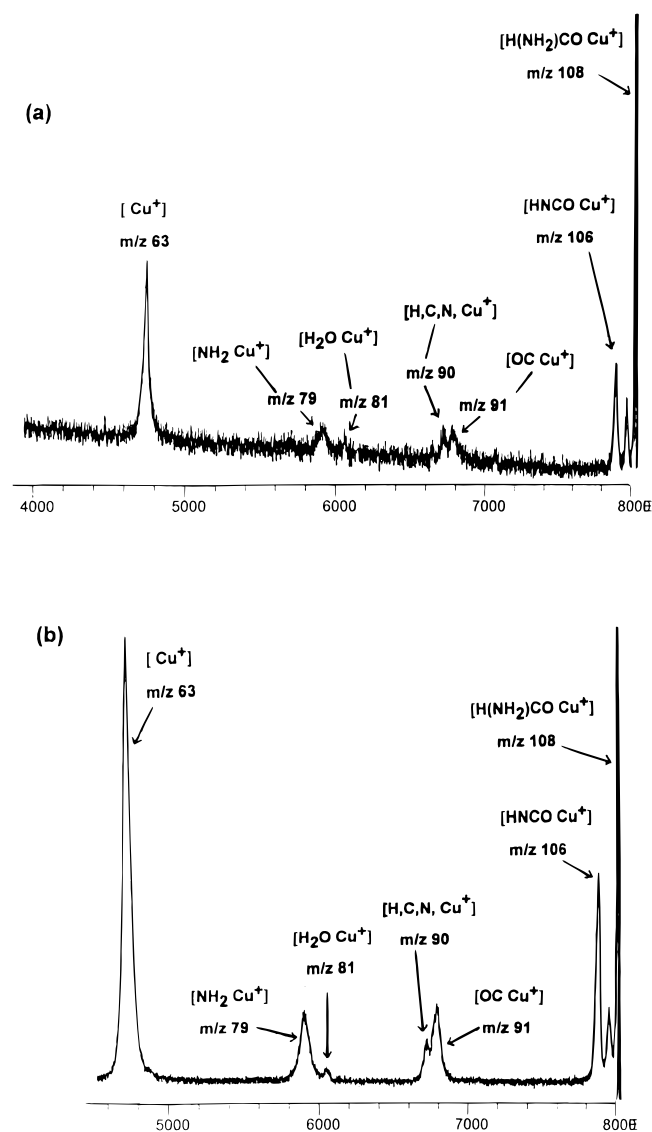
Figure 2. (a) Metastable ion mass spectrum of formamide-Cu$^+$ (*m/z* 108) and (b) CAD spectrum of formamide$-$Cu$^+$ (*m/z* 108).

since it readily dehydrogenates formamide, yielding a cluster ion [H$_2$,N,O,C,Cu$_2$]$^+$ at *m/z* 170 (29%).

MIKE analysis was performed on [formamide-Cu]$^+$, [(formamide)$_2$Cu]$^+$, [formamide-Cu$^+$-NH$_3$], and [H$_2$,N,O,C,-Cu$_2$]$^+$ adduct ions to obtain information regarding the structure, reactivity, and thermochemistry of these Cu$^+$/organic complex ions. The results presented here refer to the more abundant isotope ^{63}Cu-containing species. These different unimolecular reactions will be analyzed separately. In each case we will give a description of the experimental results, followed by a discussion, based on our DFT calculations, on the possible mechanisms. For this purpose we shall study the structures and the relative stabilities of the complexes which undergo the unimolecular decomposition, and the most outstanding characteristics of the corresponding PES.

Unimolecular Reactivity of [Formamide-Cu]$^+$ Adduct Ion. The MIKE spectrum of the [formamide-Cu]$^+$ complex presented in Figure 2a shows that the *m/z* 108 ion undergoes fragmentation by several distinct pathways. The major fragmentation corresponds to its dissociation to produce Cu$^+$ ion at *m/z* 63 (base peak of the spectrum). The [formamide-Cu]$^+$ complex ion shows other losses, namely that of H$^\bullet$ at *m/z* 107, H$_2$ at *m/z* 106, NH$_3$ at *m/z* 91, H$_2$O at *m/z* 90, and other losses of 27 and

29 u, that could correspond to HCN/HNC and HCO, respectively. The fraction of metastable ions decomposing in the second FFR is in fact very low (the main beam at *m/z* 108 and the one at *m/z* 63 are in the ratio 5 × 10^6/1), resembling rather a collision spectrum where the activation comes from collisions with background gas. To clarify this point, we have measured the CAD spectrum using Ar as a reagent collision gas. This spectrum is presented in Figure 2b. The main feature of this figure is that we can observe a selective increase of the intensities corresponding to loss of NH$_3$ (*m/z* 91) and HCO (*m/z* 79) in comparison with those of HCN/HNC and H$_2$O. This seems to indicate the existence of high barriers leading to such fragmentations, as we will discuss later in light of our theoretical results.

Dehydrogenation of [formamide-Cu]$^+$ complex via metastable or activated transient species takes place with generation of [HNCO-Cu]$^+$ ion. Interestingly, [formamide-Cu$^+$] adduct ion yields exclusively [HNCO-Cu]$^+$ species and not the alternative [H$_2$Cu]$^+$ fragment ion. As will be discussed later, this result reflects that H$_2$ is not as effective as HNCO fragment in binding Cu$^+$.

Characteristics of the [Formamide-Cu$^+$] Complexes. As mentioned above, to provide a rationale to these experimental findings we have taken advantage of our DFT calculations on the most relevant features of the corresponding PES.

The optimized geometries of the different formamide$-$Cu$^+$ complexes are shown schematically in Figure 3. They correspond to the direct association to O (**1a,b**), to N (**1c**), and to the insertion into C$-$NH$_2$ bond (**2a,b**). This figure also includes some relevant transition states. Their total energies as well as their relative stabilities have been summarized in Table 1.

The most stable formamide-Cu$^+$ complex corresponds to the attachment of the metal monocation to the carbonyl oxygen atom, which is also the most basic center with respect to other reference acids[20a] such as H$^+$, Li$^+$, Na$^+$, Mg$^+$, and Al$^+$. The oxygen attached species presents two conformers, namely **1a** and **1b**, where the metal cation is trans or cis with respect to the amino group. According to our estimations the latter is only 2.3 kcal/mol less stable than the former. A rather small interconversion barrier (1.9 kcal/mol) between both species, through structure **TS1a1b** has been also calculated. When ZPE corrections are taken into account this barrier disappears. Considering the limitations of the theoretical method used,[42] we cannot conclude whether **1b** actually exists as a real minimum of the PES but, in any case, an easy evolution to **1a** is expected.

The metal association to the amino group leads to a local minimum, **1c**, which lies 20.9 kcal/mol above the global minimum **1a**. It is worth noting that a slightly smaller energy gap (15.5 kcal/mol) has been previously reported[20a] between the oxygen and nitrogen-protonated species in formamide. Two other stationary points, namely **TS1c′** and **TS1c″** (See Figure 3)**,** where the metal cation is attached to the amino group of the base, were also located, but both of them were found to be transition states with a sole imaginary frequency which corresponds to the internal rotation of the OCH moiety. These rotation transition states lie 6.1 and 1.4 kcal/mol, respectively, above the local minimum **1c**.

The interconversion between both adducts **1b** and **1c** takes place through the **TS1b1c** transition state, which lies only 0.6 kcal/mol higher in energy than **1c** species. Similar to what happens for **TS1a1b**, this barrier disappears when including the

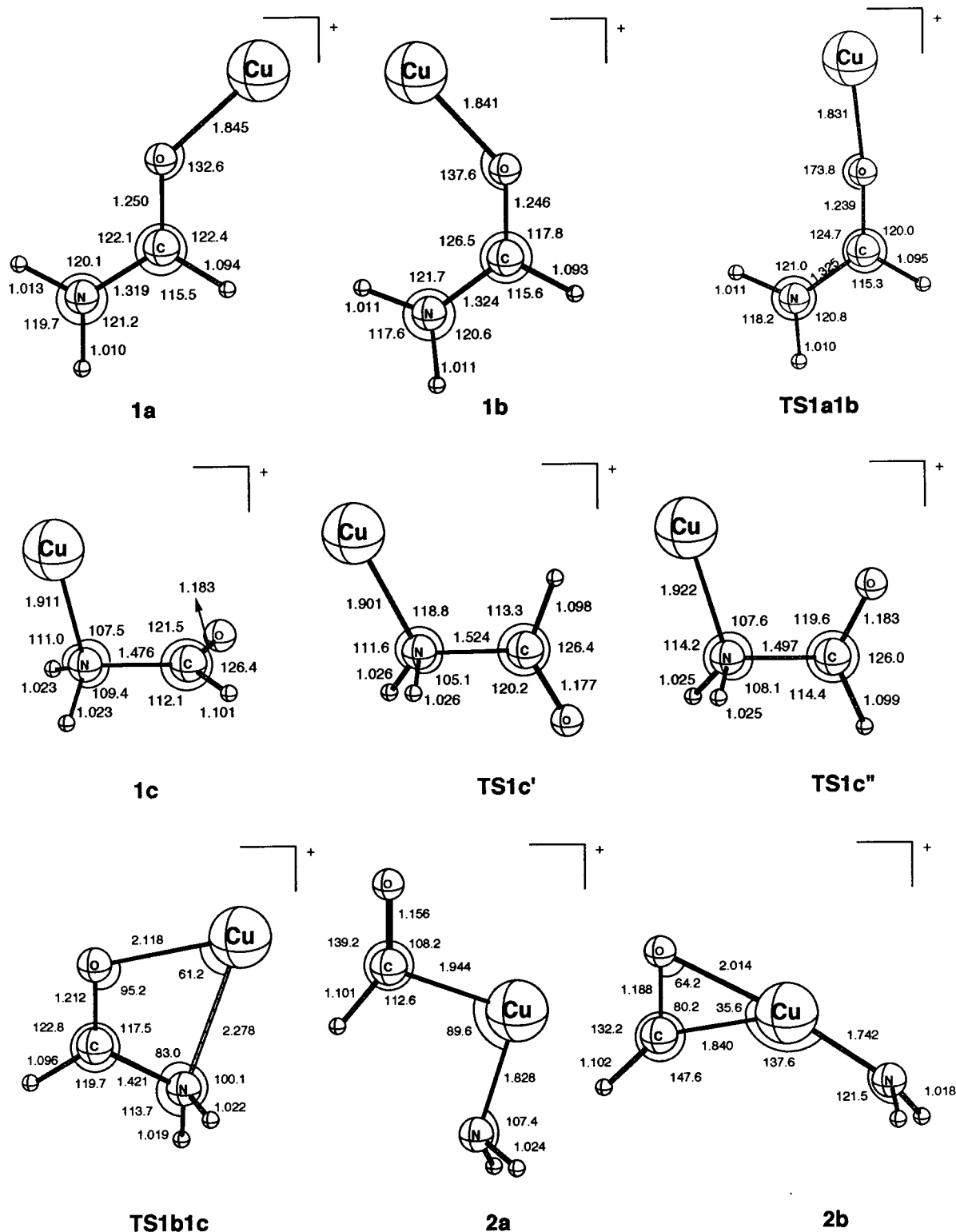(42) Luna, A.; Mebel, M.; Morokuma, K. *J. Chem. Phys.* **1996**, *105*, 3187.

Figure 3. B3LYP/6-311G(d,p)-optimized geometries of formamide−Cu$^+$ direct adducts, Cu$^+$-inserted species, and transition states involved in the transformations among direct adducts. Bond lengths are in angstroms, and bond angles, in degrees.

ZPE correction. Hence taking into account the aforementioned limitations of theoretical method used,[42] we can only predict an easy evolution from **1c** to **1b** but the existence of structure **1c** as a real minimum of the PES cannot be totally discarded. On the other hand, as we will see later, the experimental observation under collision conditions of CuNH$_2$$^{\bullet+}$ seems to indicate that **1c** species is relevant with regard to this reactivity.

The two minima (**2a,b**) corresponding to the insertion into the C−NH$_2$ bond were found to lie 12.2 and 20.7 kcal/mol above

the reactants. In other words, insertion, which has been proposed as an important mechanism in some other systems,[18] does not seem to be a relevant process in our case. Therefore, we will not consider these minima as suitable starting points to explain the reactivity in formamide−Cu$^+$ processes.

The calculated formamide−Cu$^+$ binding energy (56.2 kcal/mol) is surprisingly equal to that previously reported[34a] for ammonia, at the same level of accuracy. This implies that the oxygen−Cu$^+$ interaction is particularly stabilizing, mainly if

Table 1. B3LYP/6-311+G(2df,2p) Total Energies (E) and B3LYP/6-311G(d,p) ZPE (in Hartrees) for the Different Species under Consideration; Relative Energies,[a] ΔE (in kcal/mol), include the Corresponding ZPE Corrections

	E	ZPE	ΔE		E	ZPE	ΔE
formamide	−169.964 28	0.04531	−	**6a**	−1 866.906 88	0.08798	0.0
1a	−1 810.233 51	0.04825	0.0	**6b**	−1 866.877 24	0.08809	18.7
1b	−1 810.229 78	0.04811	2.3, 2.3[c]	**6c**	−1 866.842 87	0.08533	38.5
1c	−1 810.200 18	0.04817	20.9, 14.3,[b] 20.9[c]	**6d**	−1 866.756 79[b]	0.08556	51.0[b]
TS1c′	−1 810.116 48[b]	0.04717	20.4[b]	**6e**	−1 866.746 75[b]	0.08542	57.2[b]
TS1c″	−1 810.123 98[b]	0.04728	15.7[b]	**7a**	−3 450.150 00	0.03305	0.0
2a	−1 810.105 20	0.04251	76.9	**7b**	−3 450.143 17	0.03100	3.0
2b	−1 810.120 39	0.04411	68.4	Cu⁺	−1 640.176 69	0.00000	−
3a	−1 810.239 69	0.04607	−5.2	CO	−113.354 81	0.00506	−
3b	−1 810.273 88	0.04722	−26.0	NH₃	−56.586 39	0.03430	−
4a	−1 810.238 86	0.04369	−6.2	H₂O	−76.462 52	0.02132	−
5a	−1 810.140 06	0.04669	57.7	HNC	−93.437 25	0.01567	−
5b	−1 810.203 87	0.04820	18.6	HCO	−113.897 13	0.01292	−
5c	−1 810.207 94	0.04875	16.4	CuNH₂	−1 696.463 36	0.02408	−
TS1aD	−1 810.083 72	0.04092	89.4	Cu−NH₃⁺	−1 696.857 21	0.03892	−
TS1a1b	−1 810.229 70	0.04754	1.9, 2.4[c]	CuCO⁺	−1 753.588 96	0.00687	−
TS1b1c	−1 810.199 47	0.04649	20.3, 21.4[c]	CuOC⁺	−1 753.556 80	0.00583	−
TS1a3a	−1 810.076 65	0.04029	93.4	CuH₂O⁺	−1 716.704 44	0.02449	−
TS1a5a	−1 810.098 00	0.04079	80.3	CuCNH⁺	−1 733.709 85	0.01841	−
TS1cD	−1 809.982 90[b]	−	104.9[c]	CuNH₂⁺	−1 696.170 33	0.02408	−
TS1c5c	−1 810.073 78	0.04104	95.7	HCO+	−1 13.588 43	0.01647	−
TS3a3b	−1 810.226 44	0.04502	2.4	HNCO	−1 68.749 17	0.02134	−
TS5a5b	−1 810.134 02	0.04655	61.4	CuNHCO⁺ **8**	−1 808.990 22	0.02416	−
TS5b3b	−1 810.126 89	0.04274	63.9	HCuNHCO **9**	−1 809.849 24	0.03006	−
TS5c5b	−1 810.188 26	0.04678	27.5	CuH	−1 641.072 91	0.00470	−
TS5c4a	−1 810.115 89	0.04208	69.9	CuHCu⁺	−3 281.345 77	0.00762	−

[a] To define the relative energies we have grouped the different systems in four different sets: (i) isomers of complex **1a** and the transient species connecting them, (ii) isomers of complex **6a**, (iii) isomers of complex **7a**, and (iv) fragment products associated with the different unimolecular reactions investigated. [b] These values were obtained at the B3LYP/6-311G(d,p) level. [c] This value does not include the ZPE correction.

Table 2. Charge Densities (ρ), Laplacian of the Charge Densities ($\nabla^2\rho$), and Energy Densities ($H(\mathbf{r})$) Evaluated at the Corresponding Bond Critical Points (all values in au)

		CO	CN	CuO	CuN	Cu₁H[a]	Cu₂H[a]
formamide	ρ	0.416	0.316	−	−	−	−
	$\nabla^2\rho$	−0.261	−0.874	−	−	−	−
	$H(\mathbf{r})$	−0.705	−0.435	−	−	−	−
1a	ρ	0.372	0.349	0.108	−	−	−
	$\nabla^2\rho$	−0.307	−0.979	0.669	−	−	−
	$H(\mathbf{r})$	−0.598	−0.515	−0.016	−	−	−
6a	ρ	0.378	0.345	0.105	0.110	−	−
	$\nabla^2\rho$	−0.290	−0.971	0.683	0.521	−	−
	$H(\mathbf{r})$	−0.611	−0.507	−0.011	−0.028	−	−
7a	ρ	0.475	0.407	−	0.100	0.111	0.184
	$\nabla^2\rho$	0.242	−1.250	−	0.466	0.178	0.067
	$H(\mathbf{r})$	−0.853	−0.617	−	−0.025	−0.055	−0.065
Cu₂H⁺	ρ	−	−	−	−	0.119	0.119
	$\nabla^2\rho$	−	−	−	−	0.149	0.149
	$H(\mathbf{r})$	−	−	−	−	−0.064	−0.064

[a] Cu₁ dessignates the Cu attom directly attached to the HNCO moiety, while Cu₂ dessignates the terminal Cu atom.

one takes into account that with respect to the proton, formamide is 6 kcal/mol less basic than ammonia.[44] As we shall discuss in forthcoming sections, this result must be taken with care, in view of some of the characteristics of the MIKE spectra of the [formamide-Cu⁺-NH₃] ions.

The formation of the most stable formamide−Cu⁺ complex implies a significant charge redistribution within the formamide subunit. A comparison of the topological characteristics of the charge densities of the neutral and the complex (see Table 2) shows that Cu⁺ association leads to an activation of the carbonyl bond, while the C−N bond becomes reinforced. The formation of the new O−Cu linkage implies a charge transfer from the basic center into the Cu−O bonding region. Since oxygen is a

very electronegative atom, it recovers part of this charge by depopulating the C=O bond. Accordingly the charge density at the bond critical point decreases, its energy density becomes less negative, and the bond lengthens. This enhances the electronegativity of the carbon atom which polarizes the amino group, so that the charge is pulled into the C−N bonding region. As a result the charge at the C−N bond critical point increases, the energy density becomes more negative and the bond shortens. These changes are also reflected in the shifts of the harmonic vibrational frequencies. As shown in Table 3, upon Cu⁺ association the C=O stretch is red-shifted by 77 cm⁻¹, while the C−N stretch is blue-shifted by 106 cm⁻¹. The N−H and the C−H stretches are also affected. The former appear at lower frequencies in the complex than in the neutral, while the latter undergo a blue shift. Hence the data in Tables 2 and 3 support an increased participation of the resonance form H₂N⁺=CH−OCu.

(43) Polce, M. J.; Beranova, S.; Nold, M. J.; Wesdemiotis, C. *J. Mass Spectrom.* **1996**, *31*, 1073.

(44) Lias. S. G.; Bartmess, J. E.; Liebman, J. F.; Holmes, J. L.; Levine, R. D.; Mallard, W. J. *J. Phys. Chem. Ref. Data* **1988**, *17*, suppl. 1.

Table 3. B3LYP/6-311G(d,p) Harmonic Vibrational Frequencies (cm^{-1}) and Assignments for Formamide and Formamide−Cu⁺ **1a** Complex

formamide		**1a**	
freq	assignment	freq	assignment
3719	NH$_2$ asymmetric stretch	3678	NH$_2$ asymmetric stretch
3581	NH$_2$ symmetric stretch	3552	NH$_2$ symmetric stretch
2921	CH stretch	3087	CH stretch
1817	CO stretch + CN stretch	1740	CO stretch + CN stretch
1620	NH$_2$ scissors	1625	NH$_2$ scissors
1422	HCO bending in plane	1412	HCO bending in plane
1267	CN stretch + HNC bend	1373	CN stretch + HNC bend
1055	NH$_2$ rocking	1110	NH$_2$ rocking
1049	HCN bending out of plane	1064	HCN bending out of plane
651	C−NH$_2$ twist	711	C−NH$_2$ twisting
568	NCO bending in plane	659	NCO bending in plane
219	NH$_2$ bending out of plane	565	NH$_2$ bending out of plane
		342	Cu−O stretch
		160	CuOC bend
		103	C−OCu twist
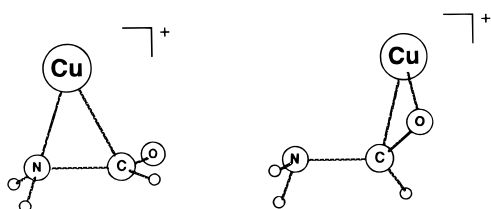
Figure 4. Formamide−Cu⁺-chelated structures investigated in this work. None of them were found to be stable.

We have also investigated the possibility of forming chelated structures where the metal cation bridges between two basic centers of the neutral. More specifically we have considered the bridged structures depicted in Figure 4. None of them have been found to be stable, as they collapsed, without activation barrier, to one of the aforementioned local minima.

Reactivity of [Formamide-Cu⁺] Complexes. As mentioned above the MIKE and CAD spectra of [formamide-Cu]⁺ complexes shows that besides the loss of the Cu⁺, H•, and H$_2$, other fragmentation processes correspond to the elimination of HCO, water, ammonia, and in a much smaller proportion, HCN and/or HNC. To gain some insight on the possible mechanisms associated with these processes we have explored the corresponding PES, which has been schematized in Figures 5 and 6. The former corresponds to those processes which originate in the oxygen adduct **1a**, while the second corresponds to those mechanisms with origins in adduct **1c**. The geometries of both minima and transition states involved in these profiles are given in Figure 7. In the present work, we have not focused our attention into the H• and H$_2$ production since they do not produce interesting information about the peptidic bond activation.

The first conspicuous feature of both PES's is that the most favorable process would correspond to the loss of Cu⁺, in agreement with the experimental evidence. Actually the energies required to dissociate either complexes **1a** or **1c** to formamide−Cu⁺ are systematically smaller than the activation barriers involved in the remaining alternative mechanisms (marked as **I** to **VII** in Figures 5 and 6). Furthermore, the mechanisms which lead to the experimentally observed loss: NH$_3$ (**I**, **II**, **III**, and **V**), HCO (**VI**), and H$_2$O and HNC (**III**) are clearly endothermic, in agreement with the low intensities of the metastable peaks associated with H$_2$O, HCO, HNC, and NH$_3$ losses.

We will start our discussion of the possible reaction paths by analyzing those originated from structure **1a** (Figure 5). The first reaction path investigated (**I**), the 1,2-H shift through the transition-state **TS1aD**, would lead to the loss of ammonia, with the formation of a COCu⁺ complex. The connectivity of this transient structure was established by means of IRC calculations.[37] In this way it was found that **TS1aD** leads, in one of the directions of the vector associated with the sole imaginary frequency to the minimum **1a**, while in the opposite direction leads to the dissociation of a molecule of ammonia.

A similar 1,2-H shift but involving the transition-state **TS1a3a** (reaction path **II**), yields a quite stable CO−Cu⁺−NH$_3$ complex **3a** (See Figure 7) which is generated via C−NH$_3$ cleavage and further reorientation of the COCu moiety. It is worth noting that this cation is 5.2 kcal/mol more stable than the adduct **1a**. This ability of Cu⁺ to dicoordinate was also found for other systems.[20a,23,24] Cu⁺ is able to form sdσ hybrids which reduce the ligand−metal repulsion[24] on both sides of Cu⁺, favoring a linear ligand−Cu⁺−ligand arrangement. This is actually the disposition of the O−Cu⁺−N bonds in complex **3a**. This complex may eventually dissociate either to COCu⁺ + NH$_3$ or to CO + CuNH$_3$⁺. Taking into account the energy gap between both dissociation limits we may conclude that evolution through the latter channel would be favored. Alternatively, the CO−Cu⁺−NH$_3$ complex may evolve through **TS3a3b,** due to the low isomerization barrier, to yield the isomer OC−Cu⁺−NH$_3$ (**3b**) which lies 20.8 kcal/mol below in energy and which may eventually dissociate also to CO + CuNH$_3$⁺ or to COCu⁺ + NH$_3$. Dissociation from structures **3a** or **3b** contrast with the nonexperimental detection of CO loss. From the inspection of the MIKE and CAD spectra (see Figure 2a,b) no loss of CO is detected. These results may be explained if one takes into account that the deposition of a large excess of internal energy into our system would favor a direct cleavage of the C−NH$_3$ bond from the **TS1a3a** transient species, rather than the reorientation of the NH$_3$ moiety leading to the species **3a**.

The third possible pathway starting from **1a** (reaction path **III**) would involve a multisteps mechanism. The first step corresponds to a 1,2-H shift through the transient species **TS1a5a** connecting **1a** and **5a**. Structure **5a** can be viewed as the association of Cu⁺ to the oxygen atom of the H$_2$N−C−OH carbene. This species easily evolves through **TS5a5b** to yield the isomer **5b** where the metal cation is attached to the carbon atom. A slightly more stable isomer of species **5b**, namely **5c**, could be identified and connected with **5b** via **TS5c5b**. Both minima **5b** and **5c** seem to be very relevant in the sense that starting from **5b**, an 1,3-H shift through **TS5b3b** would lead to the global minimum **3b** which would eventually dissociate to CO + CuNH$_3$⁺ or to NH$_3$ + Cu−CO⁺. By following similar arguments to those used in the previous paragraph, the latter dissociation should be favored under collision conditions, in agreement with the experimental observations. Starting from **5c**, a barrier of 53.5 kcal/mol (**TS5c4a**) would connect this species with the bisligated isomer HNC−Cu−OH$_2$⁺, (**4a**) which could dissociate into H$_2$O + HNCCu⁺ or into CuH$_2$O⁺ + HNC, the former being energetically favored. This is in agreement with the experimental evidence which shows that the HNCCu⁺ peak is more intense than the CuH$_2$O⁺ one. Again, under collision conditions the formation of **4a** complex can compete with the direct C−OH$_2$ cleavage. It is worth noting that HCN is predicted to be 15 kcal/mol more stable than HNC; however, starting from complex **4a** the formation of H$_2$OCu⁺ comes neccesarily from the loss of HNC.

It must be noted that along the previous discussion we have not considered any mechanism involving the local minimum
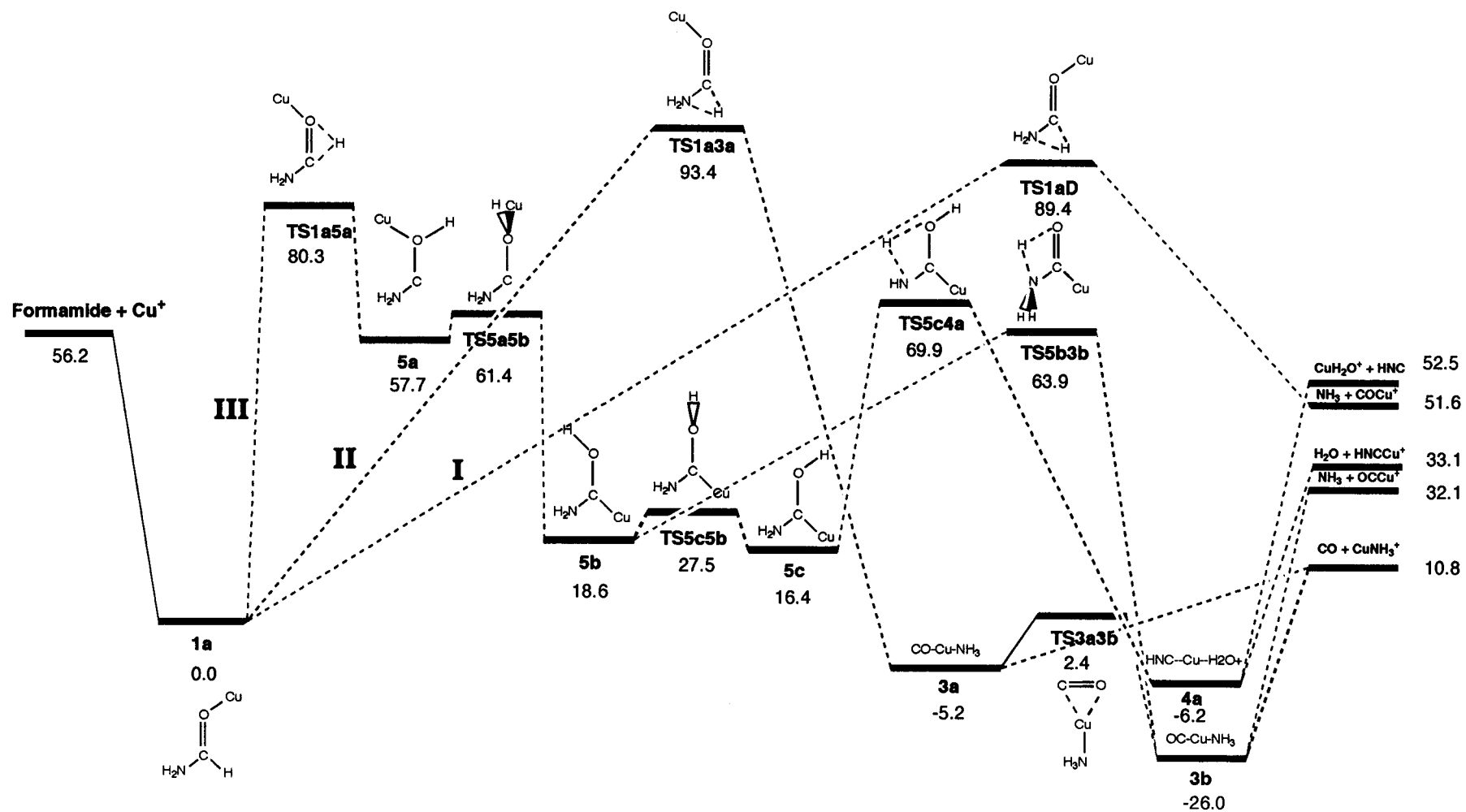
Figure 5. Schematic representation of the potential energy surface associated with the unimolecular reactions of formamide$-$Cu$^+$ complexes with origin in the most stable adduct **1a**. Relative energies are in kcal/mol.
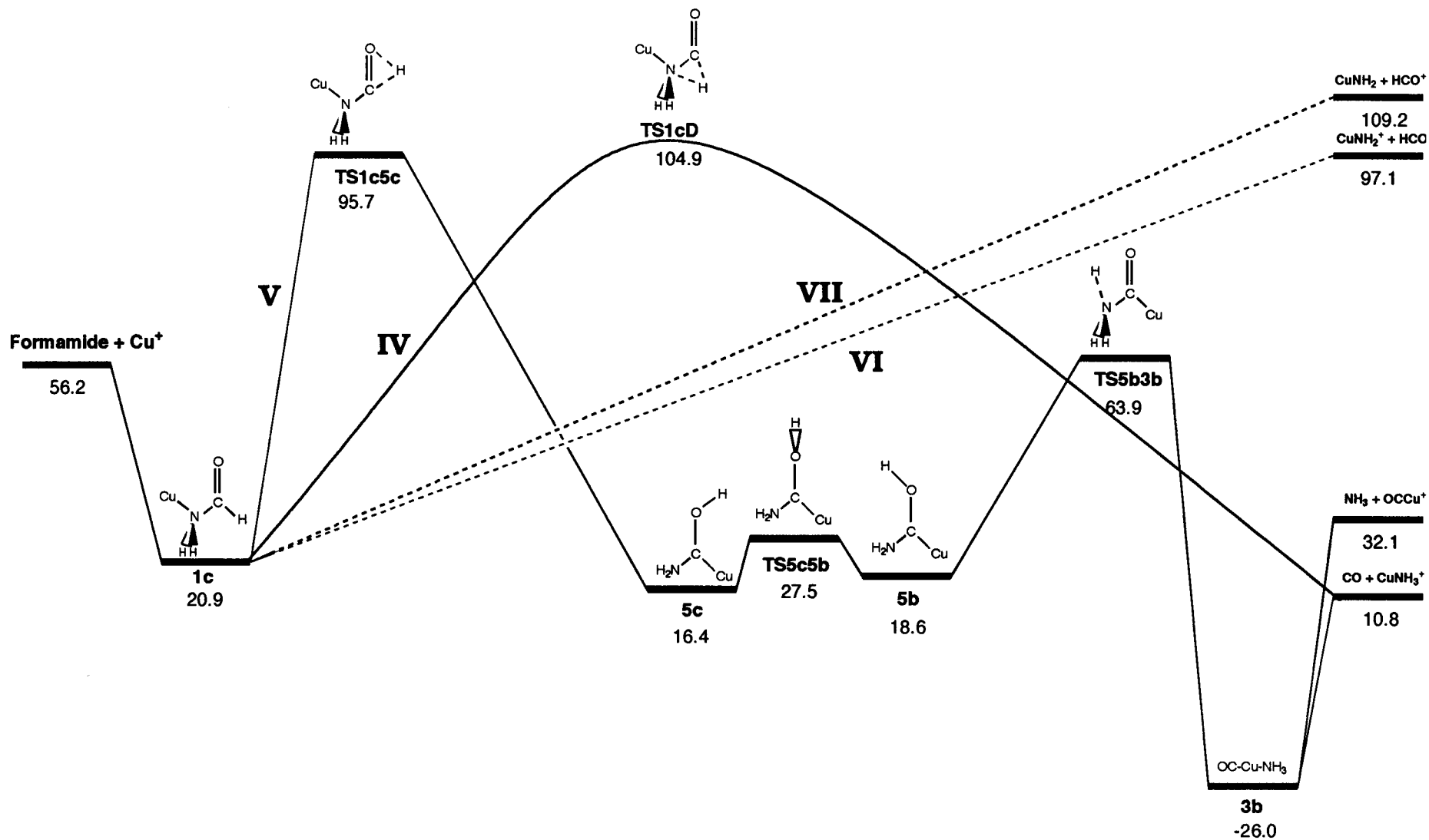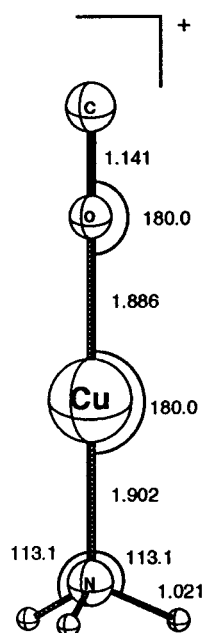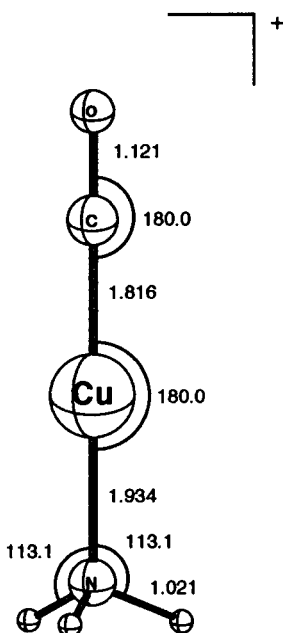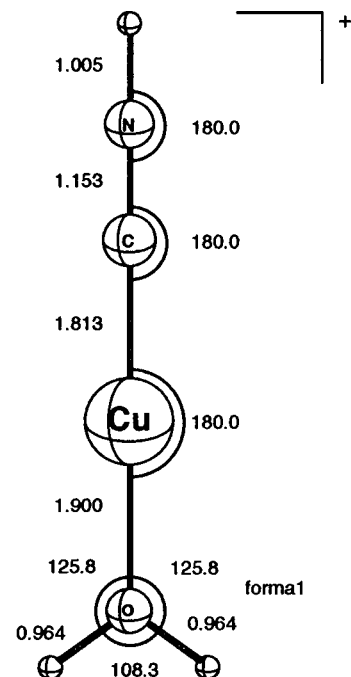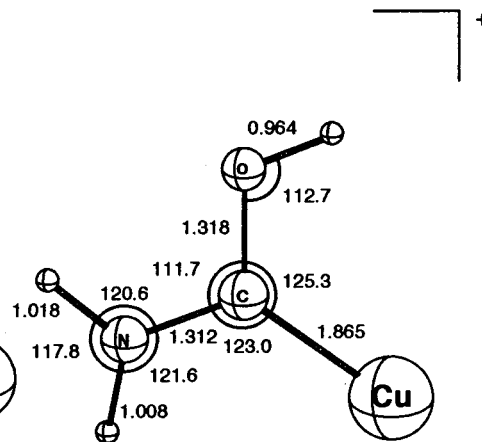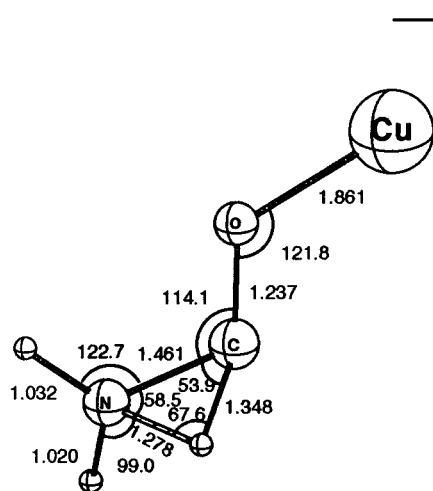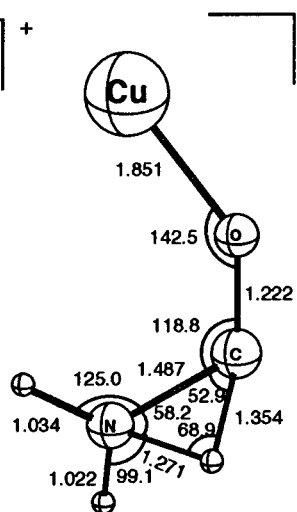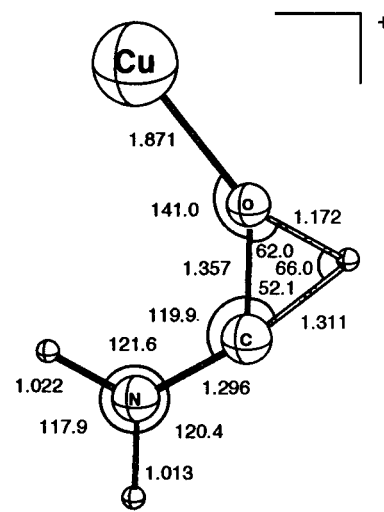
Figure 6. Schematic representation of the potential energy surface associated with the unimolecular reactions of formamide−Cu⁺ complexes with origin in the adduct **1c**. Relative energies are in kcal/mol.

Formamide−Cu⁺ Reactions in the Gas Phase

J. Am. Chem. Soc., Vol. 120, No. 22, 1998 5419

3a

3b

4a
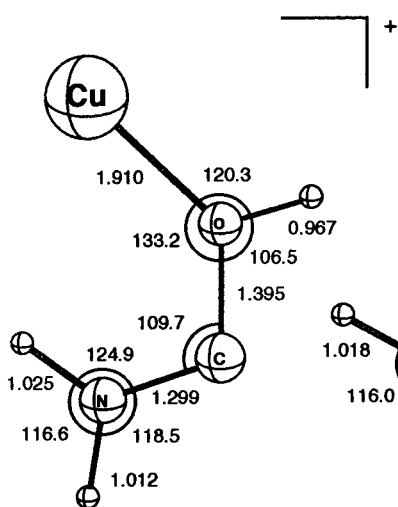
5a
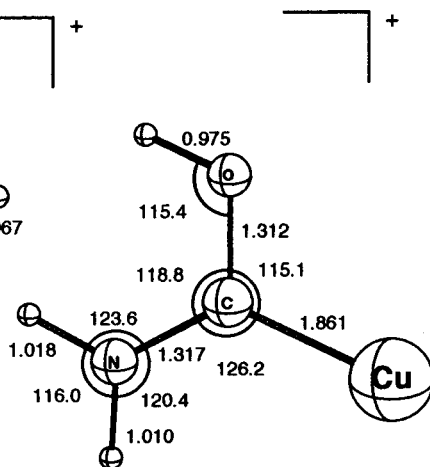
5b

5c

TS1aD

TS1a3a

TS1a5a
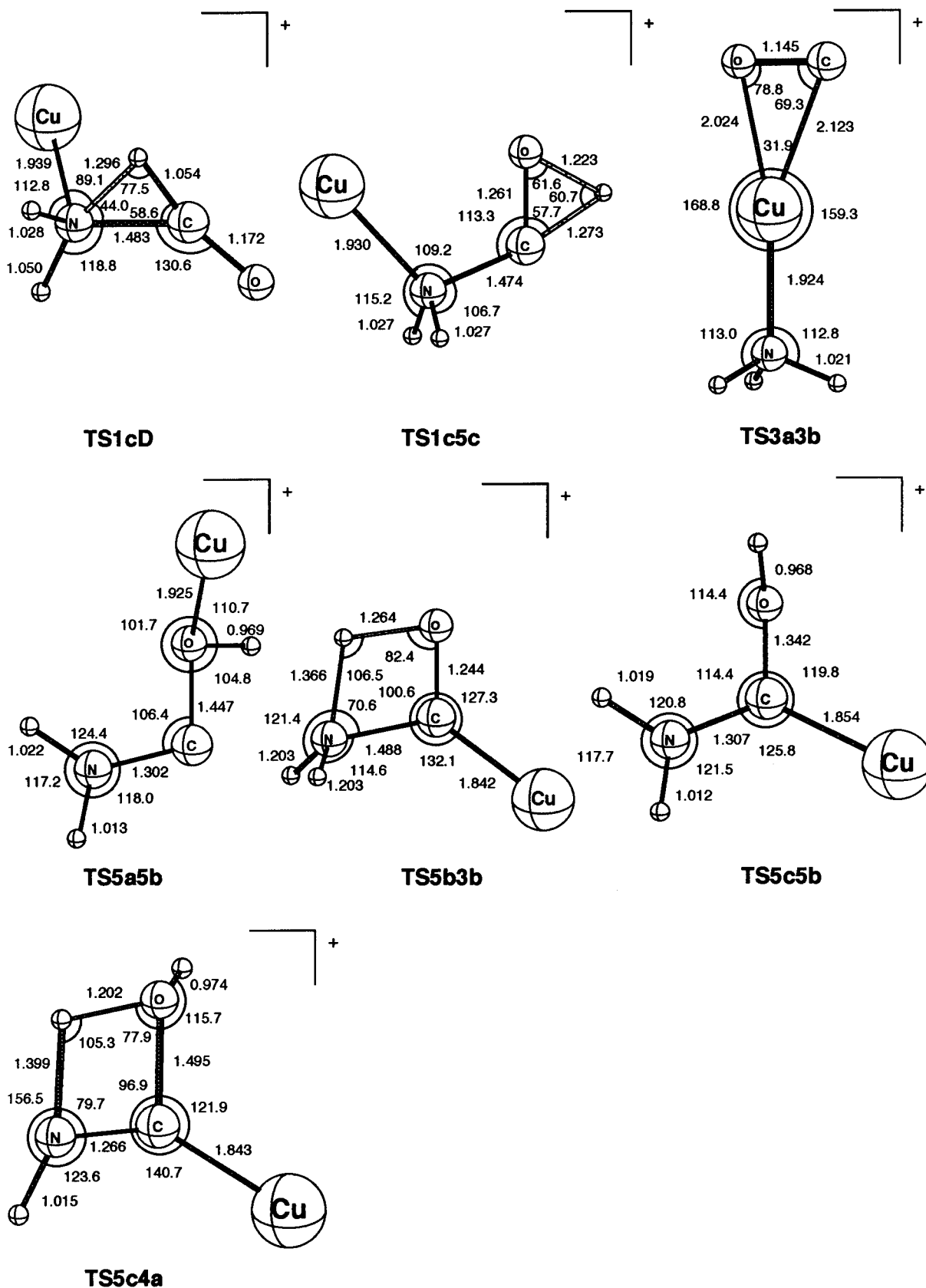
Figure 7. B3LYP/6-311G(d,p)-optimized geometries of formamide−Cu⁺ local minima and transitions states involved in the decompositions of direct adducts. Bond lengths are in angstroms, and bond angles, in degrees.

1b (see Figure 3) because of the rather small interconversion barrier (**TS1a1b**) between species **1a** and **1b**.

Alternative mechanisms (**IV** to **VII**) could have their origin in complex **1c** (see Figure 6) where Cu⁺ is attached to the amino group of formamide. Path **IV** implies a shift of the hydrogen

atom attached to the carbonyl carbon toward the amino group. All attempts to locate the transition state for this 1,2-H shift failed, because all the initially tested structures collapsed systematically to the rotation transition states **TS1c′** or **TS1c″** (see Figure 3), which, as we have already mentioned above,

are not very high in energy with respect to **1c**. Therefore we have investigated this possible mechanism by scanning the distance between the amino nitrogen and the hydrogen atom of the HCO group, which was taken as a suitable reaction coordinate. The initial value for the N⋯H distance was set equal to that in the local minimum **1c** and it was allowed to vary in steps of 0.05 Å. To locate with more precision the top of the barrier, these steps were reduced to 0.005 Å in the region around the maximum of the potential energy curve. From these calculations, carried out at the B3LYP/6-311G(d,p) level, the barrier for this hydrogen transfer (through **TS1cD**) is estimated to be 84 kcal/mol and leads to the breaking of the C−N linkage, so that the products would be CO and $CuNH_3^+$.

A second mechanism (reaction path **V**) corresponds to the formation of complex **5b**. A 1,2-H shift would connect minima **1c** and **5c** through the transient species **TS1c5c**. Apparently, this 1,2-H shift should yield a complex where the Cu^+ metal cation is attached to the amino group of the $H_2N−C−OH$ carbene. However such a complex is not stable as it collapses to structure **5c**. Complex **5c** may then evolve through a rotational barrier of 11.1 kcal/mol (**TS5c5b**) to yield species **5b**, which will follow the dissociation pathway described already above.

Finally $CuNH_2^{•+}$ can only be generated by starting from **1c** species, under collision conditions (reaction path **VI**). We propose the direct dissociation as a suitable mechanism, since it is well-known that high energy (collisional activation) conditions can activate the NC bond. In fact, the Cu^+ cationization enlarges the CN distance from 1.361 Å in neutral formamide to 1.476 Å in complex **1c**, revealing a significant activation of this bond. The alternative reaction path **VII** would yield $CuNH_2 + HCO^+$, which lies 12.1 kcal/mol higher in energy and should be less favorable.

From the previous discussion we can summarize the most important conclusions of our survey regarding the formamide−Cu^+ MIKE and CAD spectra as follows:

(i) There are seven different mechanisms which lead to the formation of the experimentally observed products, involving activation barriers between 75 and 93 kcal/mol. The three most favorable pathways, **V**, **VI**, and **III**, would be enough to explain the formation of the experimentally observed products that we intend to study. However, it must be taken into account that the first two present the lowest energetic barriers (74.8 and 76.2 kcal/mol) because they have their origin in species **1c** which lies about 20 kcal/mol above the global minimum **1a**. Hence, the remaining possible pathways, **IV, VII, I**, and **II**, which present slightly higher barriers (84.0, 88.3, 89.4, and 93.4 kcal/mol respectively), cannot be discarded as reactive channels.

(ii) Cu^+-bound heterodimers [CO-Cu^+-NH_3] or [HNC-Cu^+-OH_2] can play a crucial role as common intermediates which undergo competitive dissociations leading to the possible fragment ions. In this respect it should be mentioned that similar bisligated (or triligated) complexes have been invoked to explain the reactivity of glycine−Cu^+ [43] and guanidine−Cu^+ [20f] complexes. The main disagreement between theory and experiment refers to the dissociation of [CO-Cu^+-NH_3], since from the theoretical point of view dissociation to CO + Cu^+−NH_3 should be observed in contrast with the experimental evidence. Nevertheless, as indicated above, the loss of HCO could mask the loss of CO in the MIKE experiments, and on the other hand, under collision conditions, direct C−NH_3 cleavage mechanisms would compete with the ones leading to the formation of Cu^+-bonded heterodimers. Finally it is also important to emphasize
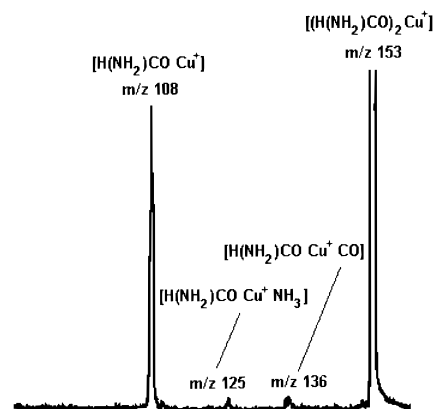

Figure 8. Metastable ion mass spectrum of [(formamide)$_2$-Cu^+] (*m/z* 153).

that the observed loss of HCO can only be theoretically explained by assuming that **1c** is a stable species.

(iii) The insertion mechanisms are not favored, while all the alternative mechanisms which can be envisaged imply at least one highly energetic 1,2-H transfer. In this respect it must be noted that 1,3- and 1,4-H transfers usually involve much lower energy barriers, as those found[20f] in the case of guanidine−Cu^+, where all barriers were energetically accessible. Taking this into account one may conclude that very likely acetamide $CH_3−C=O−(NH_2)$ would be more appropriate than formamide to model the reactivity of peptidic functions since it offers the possibility of 1,3-H transfers.

Unimolecular Reactivity of [(Formamide)$_2$Cu]$^+$ Adduct Ion. Going from [formamide-Cu]$^+$ to [(formamide)$_2$Cu]$^+$ provides the opportunity of studying the effects of subsequent ligand attachment on the chemical properties of the metal center. Figure 8 shows that the main dissociation of [(formamide)$_2$Cu]$^+$ complex via metastable transitions takes place with the generation of [formamide-Cu]$^+$ ion at *m/z* 108 (100%). Besides, two other minor fragmentations leading to the formation of [formamide-Cu^+-NH_3] ion at *m/z* 125 (4%) and [formamide-Cu^+-CO] ion at *m/z* 136 (8%) are observed. Taking into account that, as mentioned above, the [CO-Cu^+-NH_3] complexes are particularly stable, an ion−molecule reaction between this complex and neutral formamide could occur under our experimental conditions to yield a triligated [CO-Cu-NH_3,formamide]$^+$ complex, which could eventually dissociate. The existence of similar triligated complexes has been previously invoked to account for the reactivity of α-amino acids.[19,43] To confirm this hypothesis a detailed analysis of the (formamide)$_2$−Cu^+ PES at the same level of theory used for the formamide−Cu^+ PES would be required. Unfortunately this is beyond our computational capacity.

Unimolecular Reactivity of [Formamide-Cu^+-NH_3] Adduct Ion. These complexes correspond to the peak at *m/z* 125 in the spectrum of Figure 1, and the structures of the different local minima found are given in Figure 9. They can be considered either the result of attaching one molecule of ammonia to formamide−Cu^+ complexes or the result of attaching the $CuNH_3^+$ ion directly to the neutral formamide molecule. In the first case two different kinds of arrangements are possible: those where the ammonia molecule is bonded to the metal cation, **6a** and **6b** (See Figure 9), and those where the ammonia molecule forms hydrogen bond complexes with the formamide moiety, namely **6c, 6d**, and **6e**. It is worth noting that the complex where the ammonia molecule forms a hydrogen bond with the oxygen atom of the formamide moiety collapses to structure **6c**. This finding is consistent with the low
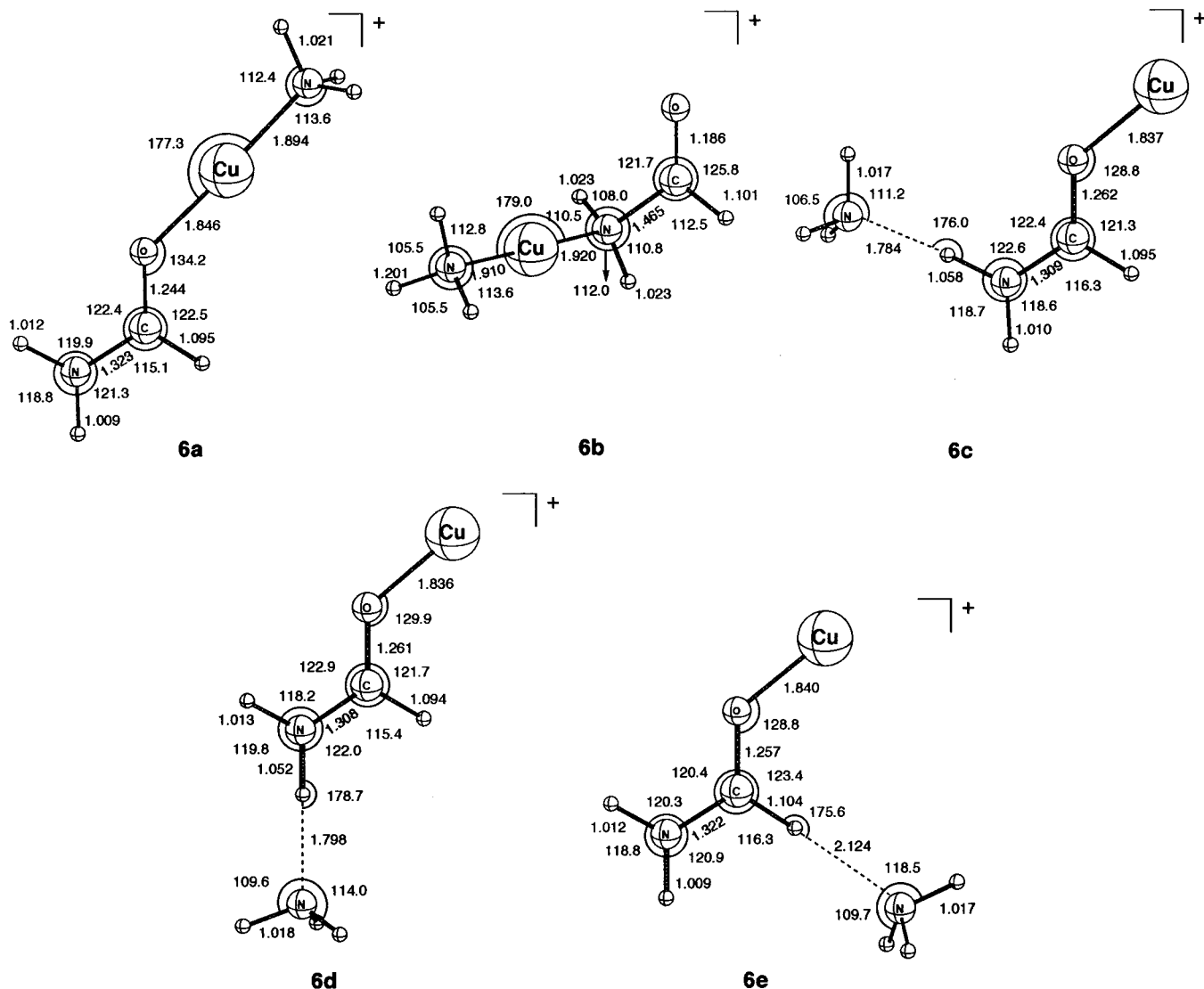
Figure 9. B3LYP/6-311G(d,p)-optimized geometries of formamide−Cu⁺−NH$_3$ complexes. Bond lengths are in angstroms, and bond angles, in degrees.

propensity of ammonia to behave as hydrogen bond donor rather than as a hydrogen-bond acceptor. The structures of the different local minima found are given in Figure 9. The corresponding energies have been summarized in Table 1. Complexes **6c−e** were found to be much less stable than complexes **6a** and **6b**, indicating that, in the latter, a strong linkage is also formed between Cu⁺ and ammonia. This shows again the ability of Cu⁺ to yield very stable dicoordinated structures, where a linear ligand−Cu⁺−ligand arrangement is favored. It is also important to realize that according to the AIM results, the formation of complex **6a** by attachment of one molecule of ammonia to the metal of complex **1a** does not perturb its charge distribution. As shown in Table 2, the charge densities at the C=O, C−N and O−Cu bond critical points of complex **6a** are rather similar to those of complex **1a**. This confirms that as was pointed out before in the literature,[20f,23,24] when Cu⁺ forms linear dicoordinated structures, the second bond does not affect in a significant way the first one.

A similar behavior is found as far as complex **6b** is concerned. This structure, which arises from the interaction of complex **1c** (where the metal cation is attached to the amino group) with NH$_3$ was found to be ~19 kcal/mol less stable than the global minimum **6a**. In other words the energy gap found between species **1a** and **1c** (~21 kcal/mol) remains practically unchanged
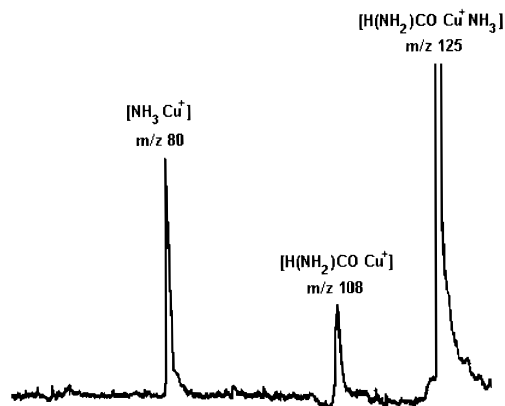

Figure 10. Metastable ion mass spectrum of [formamide-Cu⁺-NH$_3$] (*m/z* 125).

upon association with one molecule of ammonia, ratifying that the formation of the linkage between the metal cation and the ammonia molecule has a negligible effect on the stability of the other bond in which the metal cation is engaged.

The MIKE spectrum for [formamide-Cu⁺-NH$_3$] complexes presented in Figure 10 shows that they undergo fragmentation by two distinct pathways, yielding [formamide-Cu⁺] at *m/z* 108
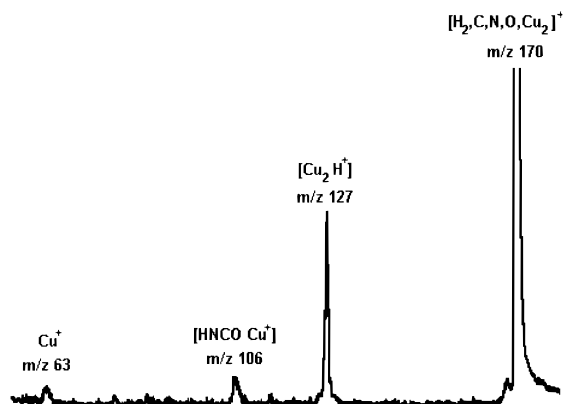
Figure 11. Metastable ion mass spectrum of [(H$_2$,N,O,C,Cu$_2$]$^+$ (*m/z* 170).

Figure 12. Optimized geometry (Å, degrees) and laplacian countour map (au) of [Cu-H-Cu]$^+$ cation. Negative values of $\nabla^2\rho$ are denoted by dashed lines and positive values by solid lines.

(50%) and [Cu$^+$-NH$_3$] at *m/z* 80 (100%) complexes. Hence, the only products observed correspond to the fission of the bonds in which the metal cation is involved. Since as we have mentioned above the Cu$^+$ binding energies to formamide and ammonia are predicted to be equal, one should expect both processes to be equally probable, i.e., one should expect the bonds between Cu$^+$ and formamide and between Cu$^+$ and ammonia to be of about equal strength. This is confirmed by the fact that the estimated dissociation energies of complex **6a** to yield **1a** + NH$_3$ or formamide + NH$_3$Cu$^+$ are equal (51.2 kcal/mol). These results do not agree, apparently, with the experimental evidence which shows that the latter process dominates. Two explanations can be invoked. On one hand, it must be taken into account that as it has been shown by Cerda and Wesdemiotis[45] for alkali metal cation complexes, the abundance ratio depends on the relative free energy of Cu$^+$ attachment to formamide vs NH$_3$, so that fragmentation in formamide + NH$_3$Cu$^+$ can be entropically favored. To investigate this possibility we have estimated the value of the $\Delta S°$ for both dissociation reactions from our DFT calculations. The results show that the entropy increment for the latter processes is 4.3 J mol^{-1} K^{-1} higher than for the former, slightly favoring indeed the dissociation of these complexes in formamide + NH$_3$Cu$^+$ in agreement with the experimental evidence.

On the other hand, it must be taken also into account that another precursor for the production of CuNH$_3$$^+$ ions is the less stable complex **6b**. As we have discussed before, the attachment of Cu$^+$ to the amino group of formamide is about 21 kcal/mol less exothermic than the attachment at the carbonyl oxygen. Therefore, in complex **6b** the linkage of the metal cation with ammonia must be significantly stronger than that with formamide, so in this case the unimolecular reaction yielding CuNH$_3$$^+$ must be strongly favored. Actually, the calculated dissociation energies of complex **6b** to yield formamide + CuNH$_3$$^+$ is 32.6 kcal/mol, while the energy required for its dissociation into **1c** + NH$_3$ is 53.4 kcal/mol.

Unimolecular Reactivity of [H$_2$,N,O,C,Cu$_2$]$^+$ Adduct Ion. The structure of this ion is not known. We are reasonably certain about the structure of complexes with one metal atom, but those with two metal atoms have several possible isomers. The fragmentation patterns may provide some insight into the structure(s) of this complex. As can be seen in the MIKE spectrum of Figure 11, dissociation of [H$_2$,N,O,C,Cu$_2$]$^+$ produces primarily [Cu$_2$H]$^+$ ion at *m/z* 127 (100%) and [HNCO-Cu]$^+$ ion at *m/z* 106 (26%). A small amount of Cu$^+$ (14%) is also observed. These results seem to indicate that these ions

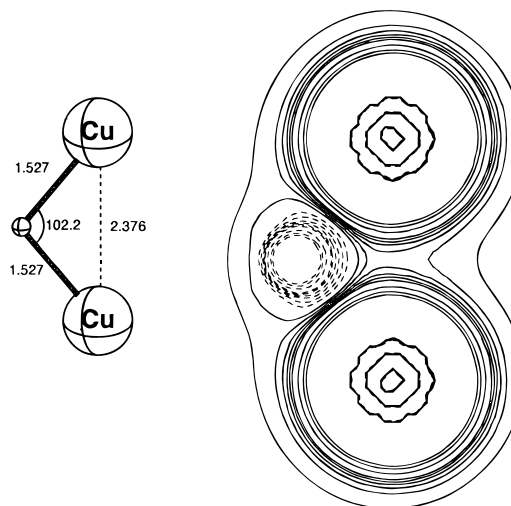are the result of the association of Cu$_2$H$^+$ clusters to a HNCO subunit, which arises from the dehydrogenation of formamide. Actually, as mentioned in previous sections, one of the peaks observed in the FAB spectra of formamide−Cu$^+$ corresponds to ions of mass 127 and 129, which are associated with [Cu$_2$,H$^+$] species according to the natural abundance of the ^{63}Cu and ^{65}Cu isotopes. Hence, the first step of our theoretical survey was concentrated on the characterization of the Cu$_2$H$^+$ species. Later we studied its possible interaction with the HNCO subunit to produce [H$_2$,N,O,C,Cu$_2$]$^+$ complexes.

Our B3LYP/6-311G(d,p) results show that the Cu$_2$H$^+$ ion has an apparent three-membered ring shape (see Figure 12). The two possible linear structures [Cu-Cu-H]$^+$ and [Cu-H-Cu]$^+$ were found to be transition states. In the first case the sole imaginary frequency (520i cm^{-1}) corresponds to a Cu−H bending while in the latter (337i cm^{-1}) it corresponds to a Cu−H−Cu bending.

To understand the bonding in this species we have analyzed the topologies of $\rho(\mathbf{r})$ and $\nabla^2\rho(\mathbf{r})$. The Laplacian map has been plotted in Figure 12, and it clearly shows a sizable charge concentration around the hydrogen. Furthermore, two bond critical points have been found between H and the two Cu atoms, whose energy densities are negative, indicating that the Cu−H interaction is essentially covalent (see Table 2). However, no bond critical point was found between both metal nuclei. Hence, we must conclude that strictly speaking [Cu$_2$,H]$^+$ species is not a three-membered ring. This bonding pattern resembles very closely that described in the literature[46] for the protonated species of P$_4$. Actually, the bonding of the hydrogen atom to the two copper atoms requires the formation of a three-center molecular orbital which arises from the in-phase interaction between the s orbital of hydrogen and the d orbitals of the appropriate symmetry of both Cu atoms (see Figure 13). The dissociation energy of this complex to yield Cu$^+$ + CuH is 58.5 kcal/mol, which is a clear indication of the strength of its Cu−H linkages.

Although several initial structures were considered for the geometry optimization of [H$_2$,N,O,C,Cu$_2$]$^+$ complexes, only two stationary points, namely **7a** and **7b** (See Figure 14), with all harmonic frequencies real were found. Their energies were included in Table 1. As anticipated above, both local minima can be viewed as the result of the association of the CuHCu$^+$

(45) Cerda, B. A.; Wesdemiotis, C. *J. Am. Chem. Soc.* **1996**, *118*, 11884.

(46) Abboud, J. L.-M.; Herreros, M.; Notario, R.; Esseffar, M.; Mó, O.; Yáñez, M. *J. Am. Chem. Soc.* **1996**, *118*, 1126.
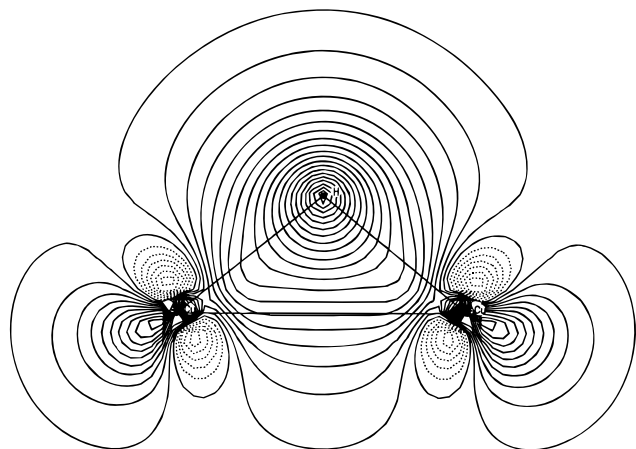
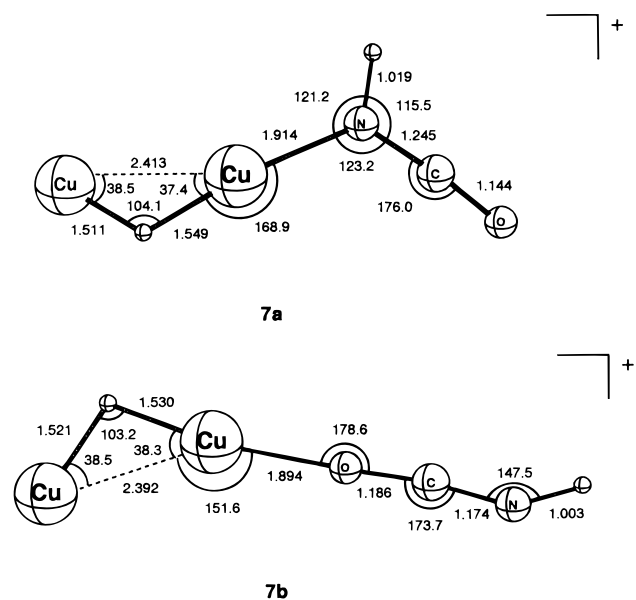**Figure 13.** Contour map of the three-center molecular orbital responsible for the bonding of the [Cu-H-Cu]$^+$ species.

Figure 14. B3LYP/6-311G(d,p)-optimized geometries of [H$_2$,C,N,O,-Cu$_2$]$^+$ complexes. Bond lengths are in angstroms, and bond angles, in degrees.

cluster formed in the source to the HNCO, which arises from the dehydrogenation of formamide, and which is the most stable isomer of the isocyanic acid. The most stable of these complexes corresponds to the attachment of the CuHCu$^+$ moiety to the nitrogen atom of the HNCO neutral system, while the association to the oxygen atom lies 3.0 kcal/mol higher in energy. We have also tried to optimize a structure where the CuHCu$^+$ subunit is attached to the carbon atom of the HNCO subunit, but it collapses to the global minimum, **7a**.

It is also worth noting that in both cases, the CuHCu$^+$ fragment retains its angular arrangement. A more detailed study of the bonding of this system reveals that as in the isolated CuHCu$^+$ cluster, the H atom is bonded to both copper atoms, even though in this case the linkages are not equivalent (see Table 2). When the CuHCu$^+$ cluster attaches to the HNCO moiety, the formation of the new N−Cu bond implies a polarization of charge into this bonding region. As a consequence, the neighboring Cu−H bond becomes depopulated and longer (see Table 2 and Figures 12 and 14), while the terminal H−Cu linkage becomes reinforced and shorter. These differences are mirrored in the peculiarities of the MIKE spectrum of species **7a**. In fact the most intense peak of the observed MIKE spectrum corresponds to the fission of the N−Cu linkage
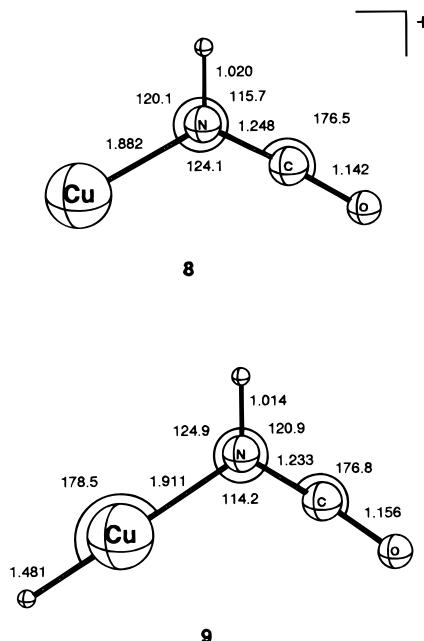

Figure 15. B3LYP/6-311G(d,p)-optimized geometries of CuNHCO$^+$ **8** and HCuNHCO **9** species formed in the unimolecular decomposition of complexes **7a** and **7b**. Bond lengths are in angstroms, and bond angles, in degrees.

which yields the CuHCu$^+$ cation. The other two are associated with the breaking of one of the Cu−H bonds of the CuHCu subunit, which, as already mentioned, have different strength. Hence, the breaking of the weakest one would yield CuH and CuNHCO$^+$ cation **8** while the breaking of the strongest one would yield Cu$^+$ and HCuNHCO neutral species **9**, in agreement with the observed abundances.

To estimate the dissociation energies involved in these processes, we have also studied, at the same level of theory, all these products. Their optimized geometries are given in Figure 15 and their energies in Table 1. From these values it can be found that in agreement with our previous discussion, the dissociation energies of complexes **7a** to yield Cu$^+$, HNCOCu$^+$ **8**, or CuHCu$^+$ are 76.0, 51.9, and 32.0 kcal/mol, respectively. Besides, these dissociation energies are consistent with the bonding characteristics discussed before and reflected by the charge densities at the corresponding bond critical points shown in Table 2. Similar dissociation processes can be envisaged from the slightly less stable **7b** complex.

It is important to emphasize that the estimated binding energy of Cu$^+$ to the HNCO moiety (38.6 kcal/mol) is almost three times larger than the binding energy for the H$_2$ molecule (14.2 kcal/mol) reported by Bauschlicher et al.[47] This is consistent with the fact, mentioned above, that no peak associated with CuH$_2$$^+$ is observed in the unimolecular decomposition of formamide−Cu$^+$ complexes, while the HNCOCu$^+$ peak is clearly detected.

Conclusions

The primary products formed in the reactions between formamide and Cu$^+$ in the gas phase, in CI−FAB conditions, correspond mainly to formamide−Cu$^+$, (formamide)$_2$Cu$^+$, for-mamide−Cu−NH$_3$$^+$, and HNCO−CuHCu$^+$ complexes. The unimolecular reactivity of these ions has been rationalized by means of a B3LYP DFT theoretical approach. This theoretical analysis shows that in formamide−Cu$^+$ complexes the attach-

(47) Maitre, P.; Bauschlicher, C. W. *J. Phys. Chem.* **1993**, *97*, 11912.

ment of Cu$^+$ takes place preferentially at the carbonyl group, while association at the amino leads to a local minimum which lies 21 kcal/mol higher in energy. The estimated formamide–Cu$^+$ binding energy (56.2 kcal/mol) is equal, at the level of theory used, to that previously reported for ammonia,[34a] although its intrinsic basicity with respect to H$^+$ is 7 kcal/mol smaller. Cu$^+$ insertions at C–N bond are energetically disfavored.

Formamide–Cu$^+$ complexes display an important feature which justifies its choice as a good starting point to provide some insights on the interactions of Cu$^+$ with the peptidic function. The attachment of Cu$^+$ to the basic centers of formamide, O or N, gives rise to the cleavage of the C–N bond through different 1,2-H shifts which are followed by rearrangements which yield bisligated complexes, where the metal cation is bonded to two neutral species, namely, CO and NH$_3$ or H$_2$O and HNC, through the formation of sd hybrids. The ability of Cu$^+$ to be dicoordinated is also corroborated by the processes which occur in the CI–FAB source yielding [(formamide)$_2$-Cu$^+$] and [formamide-Cu$^+$-NH$_3$] complexes.

It is worth noting that Freiser et al.[48] have postulated these kinds of structures to explain the reactivity of acids, esters, and ketones with Cu$^+$. Recently we have also rationalized the metastable fragmentation of guanidine[20f] by the intermediacy of bisligated Cu$^+$ complexes. There is however a very important difference between guanidine–Cu$^+$ and formamide–Cu$^+$ reactions. In the latter the formation of [CO-Cu$^+$-NH$_3$], [H$_2$O-Cu$^+$-

NCH] and [OC-Cu$^+$-NH$_3$] complexes results from highly energetic 1,2-H transfers leading to an endothermic mechanism, while in the former a 1,3-H transfer mechanism is involved so that the loss of NH$_3$ from a [HN=C=NH–Cu$^+$–NH$_3$] intermediate is exothermic. This kind of intermediates can also explain the reactivity of amino acids as postulated by Wesdemiotis et al.[43] These authors evidenced the formation of triligated [(CH$_2$=NH)–Cu$^+$–(CO)(H$_2$O)] complexes in the case of glycine–Cu$^+$ by means of neutralization–reionization techniques. The formation of this complex needs a favorable 1,4-H transfer which can explain the efficiency of the process and the loss of 46 u (H$_2$O and CO).

The fact that in formamide–Cu$^+$ reactions only highly energetic 1,2-H transfers are possible lead us to conclude that very likely acetamide would be a better model system, since it allows the possibility of 1,3-H shifts. Following the same arguments, to fully understand the reactivity of Cu$^+$ with peptides it would be necessary to consider larger systems as diglycine, where the peptidic function as well as C- and N-terminal residues are present.

(48) Burnier, R. C.; Byrd, G. D.; Freiser, B. S. *Anal. Chem.* **1980**, *52*, 1641.

JA971623O